Available online at www.sciencedirect.com
SCIENCE DIRECT®
Pergamon
Cement and Concrete Research 33 (2003) 1963–1966
CEMENT AND CONCRETE RESEARCH

Study of surface irregularity on corrosion of steel in alkaline media

Changiz Dehghanian*

Department of Chemical Engineering, University of Technology in Isfahan, P.O. Box 111, Isfahan, Iran

Received 4 August 1999; accepted 17 June 2003

Abstract

In this study, the effects of the surface condition of rebar on its cathodic current efficiency were investigated. The cathodic current efficiencies for rebar with different surface conditions were determined from cyclic polarization experiments. The results showed that cathodic faradaic current increased with surface irregularity. Surface condition of steel in alkaline solution also had an effect on double-layer capacitance.

Keywords: Concrete; Corrosion; Surface; Kinetics; Rebar

1. Introduction

Reinforcing steel bars (rebars) in concrete have initially passive surfaces because of their highly alkaline environment. Passivity may be lost locally because of chloride ion concentration or carbonation of concrete [1]. Corrosion macrocells can then develop with a considerable portion of the cathodic reaction (usually oxygen reduction) taking place on passive steel surfaces [2,3]. The condition of the metal surface (metal finish, presence of mill scale, or prior corrosion products) is expected to have an effect on the rate of the cathodic reaction. This effect is important in the long-term deterioration of a structure. In addition, surface condition may strongly influence the apparent interfacial capacity of the rebar surface. Because the apparent interfacial capacitance in concrete tends to be quite large [4–7], variations in that magnitude can introduce significant changes in the results of electrochemical corrosion rate measurements [6,7].

2. Experimental procedures

2.1. Sample preparation

Two types of rebar no. 4 were selected; one was new steel rebar (NS) and the second was a rebar that had been in a highway bridge deck for 30 years (HS). Samples of length 5 in. were cut from straight sections of the rebars. One end of each rebar was drilled and tapped with a 3/16-cm (6/32-in.) hole without using oil or water. Both ends of the rebars were coated with gray epoxy coating for 1.27 cm (1/2 in.) from the bottom and 3.175 cm (1.25 in.) from the top leaving a 8.25-cm (3.25-in.) length of rebar bare. Different surface roughness were produced on the rebars:

1. One rebar of type NS was used as received and rusted (NS-R). The rusting procedure was performed by immersing the rebar in 3.5% salt solution for few seconds and by placing it in a dry laboratory for a day. This alternate wetting and drying cycle lasted for a week.
2. One rebar of type NS was used as received (NS-AR).
3. One rebar of type HS was used as received (HS-AR).
4. One rebar of type HS was sandblasted (HS-B).
5. One rebar of type HS was sandblasted and rusted (HS-BR) as in 1.

After cleaning with distilled water to remove any residue of salt on the samples. These samples were placed in a closed tank containing saturated calcium hydroxide solution. The solution was purged with nitrogen gas to reduce oxygen content in the solution. The potential of the rebars was measured daily with respect to a saturated calomel reference electrode. When rebars showed a steady potential and passive behavior, cathodic polarization experiments were performed. Cyclic polarization was carried out from

* Tel.: +98-21-465-4703; fax: +98-21-800-6076.
E-mail address: cdehghan@ut.ac.ir (C. Dehghanian).

0008-8846/$ – see front matter © 2003 Elsevier Ltd. All rights reserved.
doi:10.1016/S0008-8846(03)00215-1

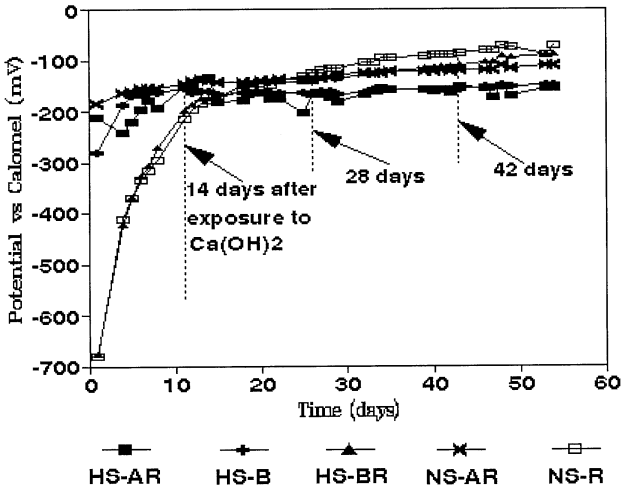

Fig. 1. Potential of rebars with different surface conditions with respect to time.

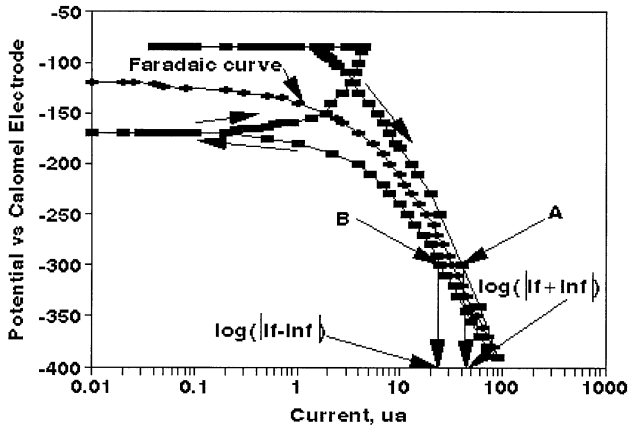

Fig. 2. A typical cyclic polarization curve with calculated faradaic curve for sample HS-B.

the open circuit potential of each sample to −400 mV (SCE). A scan rate of 0.1 mV/s was used. In the above electrochemical tests, a titanium wire mesh was placed in one side of the tank wall and used as a counterelectrode. A titanium wire was also used as a quasi-reference electrode. To check the reproducibility of the test results, five times the rebar sample potentials with the same surface treatments were measured and the same electrochemical experiments were done.

The apparatus used for cyclic cathodic polarization was a potentiostat/galvanostat (model 173) with a Wenking voltage scan generator (model 72) and Houston Instrument Recorder (model 2000).

3. Results and discussion

Fig. 1 shows a plot of potential with respect to time for the samples of different surface roughness in saturated calcium hydroxide solution. The statistical analysis for the potential measurements of the five samples with the different surface treatment is shown in Table 1. The results show reasonable standard deviation and standard error.

During the initial days of immersion, the potentials of samples HS-BR and NS-R were more negative than those of the other samples. The potential of all samples shifted toward more positive direction with time and after approximately 2 weeks, the potentials stabilized, indicating passivity in saturated calcium hydroxide solution. Similar results were observed with the duplicate samples. From the cyclic cathodic polarization curves pure faradaic cathodic currents were determined as shown in a typical cyclic cathodic polarization curve in Fig. 2. To obtain faradaic cathodic currents, the total currents for the forward and backward sections of cyclic curves at the same potential were averaged. This was done at several potentials to obtain a plot of potential with respect to the faradaic cathodic current as shown in Fig. 2. To demonstrate the reason for averaging the forward and backward currents to obtain faradaic current; consider the circuit for the metal–electrolyte interface shown in Fig. 3. The total

Table 1
Statistical analysis for potentials measurements of the five samples at 28 days of exposure to saturated calcium hydroxide solution

Sample type	HS-AR	HS-B	HS-BR	NS-AR	NS-R
Potential 1	− 165	− 175	− 145	− 140	− 118
Potential 2	− 167	− 185	− 150	− 145	− 132
Potential 3	− 170	− 185	− 160	− 138	− 126
Potential 4	− 160	− 157	− 138	− 150	− 132
Potential 5	− 171	− 178	− 141	− 134	− 140
Maximum value	− 160	− 157	− 138	− 134	− 118
Minimum value	− 171	− 185	− 160	− 150	− 140
Mean	− 166	− 176	− 146	− 141	− 129
Standard deviation	4.39	11.48	8.64	6.22	8.17
Standard error	1.96	5.13	3.86	2.78	3.65
95% confidence interval	(− 173, − 159)	(− 193, − 158)	(− 160, − 133)	(− 151, − 131)	(− 142, − 116)
Coefficient of variation	− 2.63	− 6.52	− 5.88	− 4.4	− 6.3

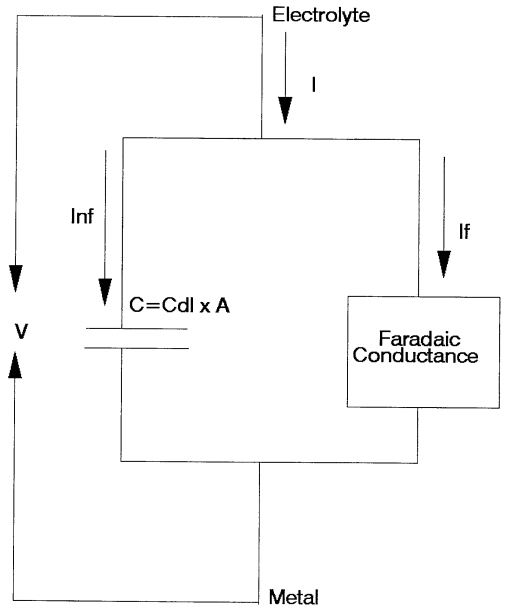

Fig. 3. Schematic of current between metal and electrolyte interface.

current (I) is I_f+I_{nf} where I_f is the faradaic current and function of voltage (V) and I_{nf} is the nonfaradaic current and defined as

$$I_{nf} = Kx\frac{dV}{dt} \tag{1}$$

in which K is a constant and dV/dt is the rate of voltage change with time. For a capacitor, $V=Q/C$, and the rate of voltage change with time across capacitor is

$$\frac{dV}{dt} = \frac{1}{C}\frac{dQ}{dt} \tag{2}$$

in which $dQ/dt=I_{nf}$, therefore,

$$\frac{dV}{dt} = \frac{I_{nf}}{C} \tag{3}$$

Comparing Eq. (1) with Eq. (3), we can conclude that $K=C$ and Eq. (1) can be written as $I_{nf}=CV$ in which V is dV/dt.

For a cathodic reaction, I_f is negative and becomes more negative as V becomes more negative. If V is becoming more negative as time increases, then dv/dt is less than zero and therefore I_{nf} is less than zero. For a cathodic reaction, I is less than I_f if the potential is going towards a more negative value and $|I|$ is greater than $|I_f|$, therefore,

$$\log|I| \phi \log(|I_f|) \tag{4}$$

The reverse will happen when the potential goes in a more positive direction. For example, in Fig. 2, the total absolute current at point A on the forward section of the cyclic polarization can be defined as log ($|I_f+I_{nf}|$) and at point B on the backward section at the same potential as A, the total absolute current is defined as log ($|I_f-I_{nf}|$). Therefore, the summation of the total absolute current at the points A and B will be $2|I_f|$ for which the average is $|I_f|$.

The faradaic current curves for each sample were determined in the same manner and the results are presented in Fig. 4. These results indicate that samples HS-BR and NS-R required the highest faradaic currents at the different cathodic potentials. The sample NS-AR required lower current than the samples HS-BR and NS-R but higher than samples HS-AR and HS-B. Sample HS-AR showed a slightly higher current than sample HS-B. Thus, samples with reduction of oxide and rougher surfaces require higher faradaic currents than samples with smoother surfaces.

The capacitance for each sample was also determined from the cyclic cathodic polarization curves. The difference in current at point A on the forward and at point B on backward portion of the cyclic polarization curve at the same potential as shown in a typical cyclic polarization curve in Fig. 2 was determined. This difference in current is defined as:

$$\Delta I = I_A - I_B = 2I_{nf} = 2CV \tag{5}$$

Therefore,

$$C = \frac{\Delta I}{2V} \tag{6}$$

or the double-layer capacitance per unit area is defined as

$$c_{dl} = \frac{C}{A} = \frac{\Delta I}{2AV} \tag{7}$$

In the above equation, V is a scan rate of the cyclic polarization curve and C_{dl} is the double-layer capacitance per unit area. A plot of cathodic current efficiencies with respect to the capacitance that was determined by the above method is shown in Fig. 5. The faradaic cathodic current densities were obtained at -390 mV (SCE). The results in this figure show that samples NS-R and HS-BR have much

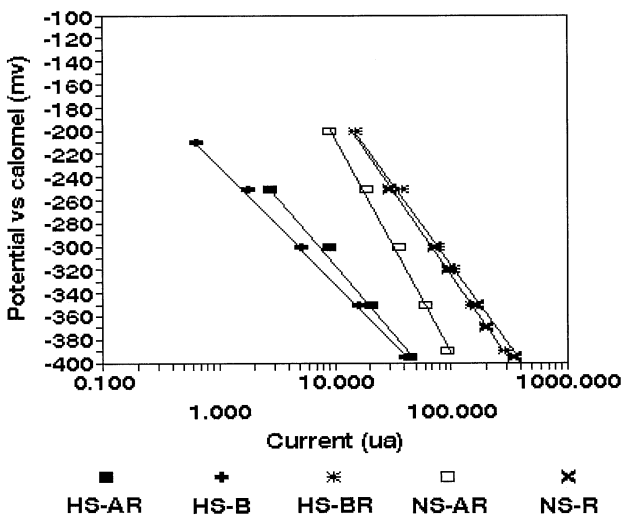

Fig. 4. Potential with respect to faradaic current.

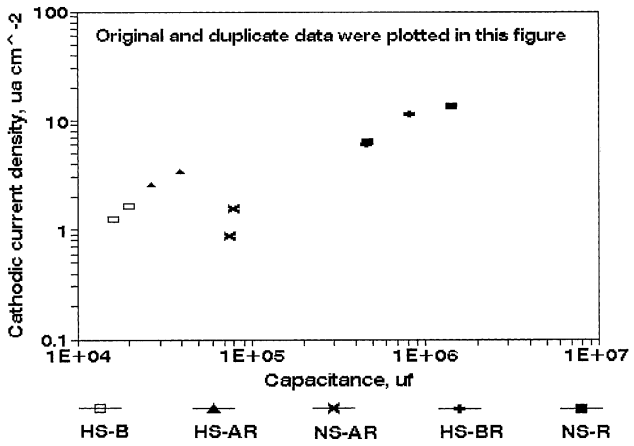

Fig. 5. Cathodic current density at − 390 mV with respect to capacitance.

higher capacitance than the other samples. Sample HS-B shows the lowest capacitance. Therefore, as surfaces become rougher and reduction of oxide takes place, the capacitance deviates from an ideal to a nonideal situation. Differences in double-layer capacitance and cathodic faradaic current for prerusted samples in comparison to samples without prerusting could partly be due to reduction of oxide. Samples without prerusting, such as NS-AR, HS-AR, and HS-B, showed different behaviors but not to the extent observed for prerusting samples. Therefore, these results confirm that both reduction of oxide and irregularity on steel surface plays an important role in electrochemical behavior of steel in alkaline environments.

In some other studies with concrete, we found the values of double-layer capacitance for rebar to be high (in the range of 3000 $\mu F/cm^2$), which contradicts with the value of 50–100 $\mu F/cm^2$ that is expected [8]. This can be understood in the light of the results presented in this article. The double-layer capacitance for even the smoothest sample HS-B was in the range of 16,000 $\mu F/cm^2$. This indicates that due to some residual surface irregularity even the sandblasted sample still has high double-layer capacitance.

4. Conclusion

1. After 14 days of exposure to saturated calcium hydroxide solutions, all samples potential were stabilized between − 100 and 200 mV (SCE), which is an indication of passivity.
2. The surface condition of the rebar in alkaline media, such as concrete, has a profound effect on the double-layer capacitance between the rebar and its surroundings. With an increase in surface irregularity, the capacitance increased tremendously.
3. The cathodic current efficiency of rebar in alkaline media increased with the roughness of the surface. Cathodic faradaic currents for samples HS-BR and NS-R were higher than other samples at each potential. Therefore, differences in cathodic performance of samples could partly be due to the reduction of oxide rather than oxygen in the cathodic reactions of macrocells.

Therefore, in studying the corrosion kinetics of a rebar in alkaline environments, such as concrete, with cyclic polarization techniques, the effect of surface condition on the parameters of the system has to be taken into consideration to avoid misinterpretation of the results.

Acknowledgements

The author would like to acknowledge the cooperation of A.A. Sagues on this research and thank the University of South Florida for providing the laboratory and equipment for carrying out this research.

References

[1] J. Slater, Corrosion of metals in association with concrete, ASTM Spec. Tech. Publ. (1983) 818.
[2] A. Aguilar, A.A. Sagues, R.G. Powers, Corrosion measurement of reinforcing steel in partially submerged concrete slabs, ASTM Spec. Tech. Publ. (1990) 1065.
[3] A.A. Sagues, H.M. Perez-Duran, R.G. Powers, Corrosion performance of epoxy-coated reinforcing steel in marine substructure service, Corrosion/91 (1991) (NACE Meetings).
[4] J. Dawson, Corrosion monitoring of steel in concrete, in: A. Crane (Ed.), Corrosion of Reinforcement in Concrete Construction, Ellis Horwood, Chichester, 1983.
[5] D. Macdonald, M. McKubre, M. Urquidi-Macdonald, Theoretical assessment of Ac-impedance spectroscopy for detecting corrosion of rebar in reinforced concrete, Corrosion 44 (1988).
[6] D. Macdonald, Theoretical analysis of electrochemical impedance, Corrosion/87 (1987) (NACE Meetings).
[7] A.A. Sagues, Critical issues in electrochemical corrosion measurement techniques for steel in concrete, Corrosion/91 (1991) (NACE Meetings).
[8] A. Sagues, Electrochemical impedance of corrosion macrocells on reinforcing steel in concrete, Corrosion/90 (1990) (NACE Meetings).